WATER-VAPOUR CHANNEL WINDS FROM SYNTHETIC RADIANCES

R W Lunnon and A D Gairey

Meteorological Office, London Road,
Bracknell, Berkshire RG12 2SZ, U.K.

ABSTRACT

METEOSAT water vapour channel radiances have been generated from objectively analysed temperature and humidity fields obtained from FRONTS87 dropsoundings. In addition, radiances a short time later were generated by applying an artificial wind field (wind speed a linear function of temperature) to the temperature and humidity data, and from the two sets of radiances, winds were retrieved using cross-correlation techniques.

For cases where there are two peaks in the histogram of radiances and a single peak in the correlation surface, the winds are very consistent, and it is found that the retrieved wind is well correlated with the mean radiance of the distribution. Thus given the linear dependence of the imposed wind field on temperature, we have the basis for a height attribution algorithm for real winds.

In addition an analytical expression has been derived for the weighting function which prescribes how the retrieved wind depends on winds at different levels. The use of such an approach is essential for the utilisation of the winds in variational assimilation.

1. Introduction

The potential for determining wind vectors by tracking water vapour structures in geostationary satellite imagery was first demonstrated by Eigenwillig and Fischer (1982), although earlier authors tracked combinations of cloud and water-vapour structures. The most recent papers on the subject are those by Laurent (1993) and Szantai (1991). Both of these authors compared their winds with "ground truth" in the form of either radiosonde ascents or numerical model data. The limitation of such an approach is that the difference between the retrieved wind and the ground truth value may stem from a number of different physical factors, so many that improving the retrieval process by simply using such comparisons would be extremely difficult. A further limitation is that a priori it is not clear what a water vapour wind should be compared with: it is well recognised that such winds are indicative of winds throughout some depth of the atmosphere. It does not even follow rigorously from theory that such winds are a weighted mean of winds throughout some depth, so an empirical search for dependency would be rather long and, given the number of other causes of difference between the two types of winds, quite possibly fruitless.

With synthetic retrievals, physical complexity can be built up in a controlled manner so that, among other things, the magnitude of the effect of each mechanism can be determined. The purpose of this exercise is to gain *understanding* of the retrieval process, which usefully supplements the information obtained using real retrievals.

Notwithstanding the consideration that water vapour winds are not representative of flow at a single level, much of the present work is aimed at answering the question: if water vapour channel winds are to be compared with single level winds, what should that level be? The method is described in section 2, results for a single case of particular interest given in section 3, and more general results given in section 4. In section 5 a theoretical framework for determining the notional weights is set down, and in section 6 required further work is described.

2. The method

In the simulation, it was necessary to specify a 2-dimensional distribution of temperature and humidity in the vertical and horizontal, and then apply a specified wind field so that the distribution at a later time can be determined. In this study the 2-dimensional distributions were derived from dropsonde data obtained in the Mesoscale Frontal Dynamics Project/FRONTS87 experiment. The experiment, the basic characteristics of the dropsonde data and the analysis technique used are described in Thorpe and Clough (1991). Briefly, the experiment consisted of flying a number of straight runs roughly perpendicular to and transecting cold fronts, dropping dropsondes at intervals. The individual runs were objectively analysed to create the 2-dimensional arrays of pressure, temperature, and relative humidity used in this study. The grid spacing of the arrays was 250m in the vertical and 10km in the horizontal. Compared to the original dropsonde data, this represents enhanced horizontal resolution but degraded vertical resolution. The telemetry on the dropsonde reports every 10s (approximately 60M) although the response time of the humidity sensor is somewhat slower than this. Given that the model atmospheres used for radiative transfer calculations (Lunnon et al (1992), although the final radiances were obtained by tri-linear interpolation between different model atmospheres) require the mean relative humidity for only three slabs, the vertical resolution of the analysed data is perfectly adequate. In the horizontal the closest separation of the dropsondes was about 30km: however a horizontal resolution of 10km is very convenient as this is almost exactly the north-south separation of METEOSAT infra-red pixels at these latitudes.
The particular advantages of the analysed dropsonde data are

- High horizontal resolution, compared to, say, radiosonde data or all but the highest resolution numerical model
- Physical realism, as opposed to simulated data
- Because they are representative of cold fronts, strong humidity gradients are present which would make good features for tracking

The limitations of the dropsonde data include

- Limited horizontal extent - the shortest leg in the analysed data had just 24 points in the horizontal which made retrievals impossible
- Limited horizontal resolution of basic dropsoundings which means that the correlations of the analysed data may be spuriously high
- Limited representivity of all meteorological situations likely to be found in the METEOSAT field of view
- Limited vertical extent. The analysed data extended from the surface to 7km altitude. There is no doubt that water vapour at higher altitudes affects

radiances at the wavelength of the water vapour channel. This is the most serious limitation of the dataset. However, the technique developed for utilising the data minimises the effects of this.

In the initial experiments, the imposed wind field was horizontally uniform, with the wind speed a linear function of height. Given that the analysed data were on a regular grid with height as the vertical coordinate, this was a rather convenient approach. However, it was decided that it was more appropriate for the imposed wind speed to be a linear function of temperature - the justification for this is given in section 5. However, the problem was that the analysed dataset did not specify the humidity at certain temperature levels at certain grid points because those temperature levels occured at altitudes above 7km. When the lower temperature limit was set so that the humidity was defined at all grid points, the resulting radiances were, not surprizingly, rather inconsistent with those obtained using height as the vertical coordinate. Therefore the approach adopted was that all profiles were extended upward to the -46°C level by
(a) Using a standard profile to obtain the pressure from the temperature
(b) Assuming that the *relative* humidity at the highest analysed level pertained at all levels above it. Given that relative humidity shows reasonable vertical correlation, this is not too bad an assumption. -46°C was chosen because it was the coldest temperature found in the data set. Although water vapour at lower temperatures undoubtedly contributes radiatively, because the selection of model atmosphere depends on layer mean relative humidities, lack of information about the humidities at these low temperatures is not critical.

The procedure then was to reanalyse the temperature, pressure and humidity data as outlined above and then impose a wind field such that wind speed was a linear function of temperature and calculate radiances at various times. The radiances were for the WV1 sensor on METEOSAT 4, using the published spectral response (ESOC, 1989). These radiances were then used to generate correlation surfaces, from which winds were generated. For IOP8RUN3 these activities are illustrated in the following section. Note that data from all six IOPs [Intensive Observing Periods] for which dropsondes were deployed were used.

It was decided to use a template size of 16 "pixels" in the retrievals, and the wind shear imposed was such that the search area was a little over 32 pixels. Therefore from a dataset with more than 32 points it was possible to generate more than one wind, and this property was exploited in order to assess the variation of retrieved wind along a continuous line.

3. Results from IOP8RUN3

Figures 1(a) to 1(d) illustrate the process of generating a wind from the aircraft data for IOP8RUN3, which was chosen primarily because it was the longest dropsonde leg, having 82 points in the dataset. Figure 1(a) shows the cross-section of humidity and temperature with height as the vertical coordinate. Figure 1(b) shows the cross-section of humidity with temperature as the vertical coordinate - the effect of assuming that the relative humidity at 7km pertains at all levels above it can clearly be seen. Also shown are ridges in the correlation surface - see below. As noted above it is possible to generate a number of winds by selecting different templates from the basic data. For overlapping templates, clearly the correlation surfaces will be rather similar, so it was decided to combine a number of correlation surfaces into a single diagram, which is figure 1(c). In this figure the x- coordinate indicates the position of the template within the complete data set of radiances, while the

y-coordinate indicates position within the search area. Thus we are seeking maxima with respect to y, and these maxima are marked by the dashed lines. The point being made is that while the correlation surface is a continuous function of x, the positions of the maxima sometimes undergo discontinuous changes. The ridges are reproduced on figure 1(b), using the prescribed relationship between temperature and wind, although because each point in the x-direction of figure 1(c) relates to a range of positions, the x-coordinates of the ridge lines are not fully defined. It becomes clear that the three ridges indicated by the three separate lines correspond to different features of the humidity field. The leftmost line relates to humidity variations at about the -30°C level in the leftmost third of the figure, the central line relates to the very strong humidity gradient in the centre of the figure at high temperatures, and the rightmost line relates to gradients at low temperatures in the rightmost third of the figure. In figure 1(d) radiance histograms are shown for the x-coordinates specified in figure 1(c). Of course the radiance histograms are continuous, as would any quantity derived from the statistical distribution of radiances. The radiances are in $Wm^{-2}sr^{-1}$.

The conclusion of this part of the study is that multiple peaks in the correlation surface can genuinely reflect motions at different levels. If it were possible to be confident that all peaks in a *real* correlation surface were genuine and not the result of aliasing, then it might be useful to average over the peaks to produce a reliable wind. However, discriminating between true peaks and aliases is rather difficult and a safer strategy is to discard correlation surfaces with multiple peaks.

4. General results from all dropsonde legs

The aim was to generate a regression relationship between a mean radiance and a temperature representative of the wind. Visual inspection of diagrams analagous to figures 1(c) and 1(d) for other IOPs and runs suggested that a reliable relationship was likely if cases where there were multiple peaks in the correlation surface or the number of peaks in the histogram was other than two, were eliminated. This is illustrated in figures 2(a) and 2(b). In the former, we plot temperature of retrieved wind against mean radiance for all IOP runs having more than 40 points (15 runs in all). As can be seen, there is considerable scatter, particularly for high radiances. In figure 2(b) the criteria specified above are applied, with IOP8 RUNs 3 and 4 eliminated in their entirety. This shows a much more linear relationship, and it was the data plotted on this figure that was used to generate statistics that follow.

In order that the concepts of a single peak in the correlation surface and two peaks in the radiance histogram are properly defined, it is necessary to specify the discretisation used. Correlation was discretised to 0.001, and the radiance histograms were generated with "bins" 0.025 $Wm^{-2}sr^{-1}$ wide. Some justification can be provided for the concept of two peaks in the radiance histogram. If there are two peaks, given that clear air radiances are a continuous function of position it implies that somewhere in spatial domain there is at least one moist area, and somewhere at least one dry area, with at least one area of sharp humidity gradient, which can be tracked.

There is some interest in comparing alternative methods of computing the radiance which is used as the basis of the height assignment. Given the existence of two peaks in the histogram, there is some plausibility attached to the concept that the mean radiance of the cluster having the lower temperature is a good indicator of the level of the wind. This was assessed (method (a) in table 1), as was the

mean radiance of the cluster having the higher temperature (method (b)), and the sum of those two radiances (method(c)). The latter might be better than considering the mean radiance of the entire histogram (method (d)) because it should be independent of the numbers of pixels in the two clusters. In addition, the mean radiance of the lowest 20% of the radiances was tried - this approach was used by Laurent (1993) although it is acknowledged that his interest was primarily in generating winds in cloudy air (method (e)).

Table 1. Statistics of temperature versus radiance algorithms

(a)	Temperature = -54.1 + 22.9 * radiance.	Correlation coefficient = .75
(b)	Temperature = -40.0 - 3.4 * radiance.	Correlation coefficient = -.27
(c)	Temperature = -43.0 + 1.2 * radiance.	Correlation coefficient = .05
(d)	Temperature = -54.9 + 23.1 * radiance.	Correlation coefficient = .90
(e)	Temperature = -52.3 + 21.1 * radiance.	Correlation coefficient = .75

As can be clearly seen, method (d), using the mean radiance of the entire histogram, works best. Note that statistics were calculated using alternatively radiances from the template and radiances from the search area, but they were very similar: the statistics in table 1 are for the template, although the data presented in figures 2(a) and 2(b) are for the search area. For method (d), the RMS error of the wind temperature derived using the regression equation above was 0.6°C. This is an encouragingly small value, implying that the height attribution error of clear air water vapour channel winds is extreemly small. However, part of the smallness can be attributed to the method of vertically extending the humidity profiles, which imposes unnaturally high vertical correlation.

5. Theoretical framework

The theoretical basis of water vapour channel wind determination starts from the radiative transfer equation, which for a single frequency can be written

$$R = \int_0^1 B \, d\tau$$

where R is the radiance at the top of the atmosphere, B is the planck function at that frequency and the temperature of the level where the transmittance to space is τ. This equation is then integrated by parts to give

$$R = \int_{B=B_{trop}}^{B=B_{b.l.}} \tau \, dB + B_{trop}$$

where B_{trop} is the planck function at the level where $\tau = 1$, (*very* approximately the tropopause) and $B_{b.l.}$ is the planck function at the level where $\tau = 0$ (usually at or somewhat above the planetary boundary layer). If it were possible to ignore the effects of water vapour at temperatures below some well defined threshold (because at that temperature the amount of water vapour the atmosphere can contain is infinitesmal), and if the temperature of the tropopause were well below that value, and if absorption due to water vapour in the stratosphere could be ignored, then we could set B_{trop} to the planck function at that threshold temperature, which would be assumed to be constant. Although the three foregoing assumptions are all open to challenge, it is reasonable to suppose that

variability of the B_{trop} term on the time and space scales relevant to water vapour wind extraction is rather small, i.e.

$$\partial R/\partial t \cong \partial/\partial t\left\{\int_{B=B_{trop}}^{B=B_{b.l.}} \tau \, dB\right\} \quad , \qquad \partial R/\partial x \cong \partial/\partial x\left\{\int_{B=B_{trop}}^{B=B_{b.l.}} \tau \, dB\right\}$$

If we now assume that temporal changes are caused by advection, so we can write

$$\partial\phi/\partial t = - u \, \partial\phi/\partial x,$$

where ϕ is any arbitrary scalar. Note that this relationship does not apply directly to τ, which arises from a vertical integral. However, correct treatment of this problem does not affect the ability to generate an analytic expression for the weighting function, merely its complexity.

Further we will assume that flow is parallel to temperature surfaces: it is acknowleged that in general adiabatic flow is parallel to potential temperature surfaces, but if we assume that flow is along isobaric surfaces, then temperature will be conserved. This allows us to use x and B as independent axes, which in turn allows commutation of the operators integration with respect to B and differentiation with respect to x. Defining the wind that results from the retrieval process as U then

$$U = {}^{\partial R/\partial x}/_{\partial R/\partial x}, \text{ whence}$$

$$U = \frac{\left\{\int_{B=B_{trop}}^{B=B_{b.l.}} u \, \partial\tau/\partial x \, dB\right\}}{\left\{\int_{B=B_{trop}}^{B=B_{b.l.}} \partial\tau/\partial x \, dB\right\}}$$

The value of this equation is that it gives an analytic expression for the weighting function in terms of variables which could certainly be calculated using the analysed dropsonde data. Thus it would not be neccessary to impose an arbitrary wind field. A wind vector together with a weighting function is the preferred form for data presentation to variational assimilation.

6. Required further research

Clearly it is highly desirable to exploit the formula for the weighting function given in the previous section. Note that calculating the weighting function from data available generally e.g. satellite radiances, numerical model forecasts, will prove a considerable challenge.

In addition it is desirable to introduce more realism into the simulations. Radiometric noise and vertical motion are two leading candidates for addition to the current system.

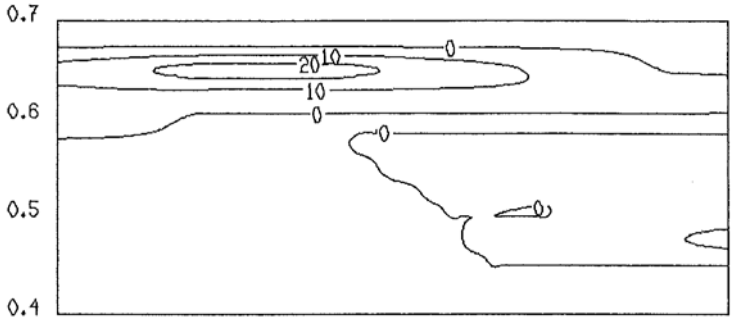

Figure 1(d). Shows histogram of radiances (y-coordinate) plotted against the same x-coordinate as figure 1(c).

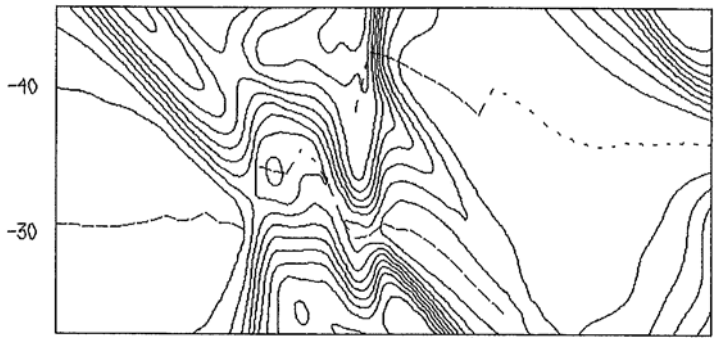

Figure 1(c) Shows correlation surface and ridges therin (dashed lines). The y-coordinate is displacement of template within the search area, the x-coordinate is position of template within cross-section.

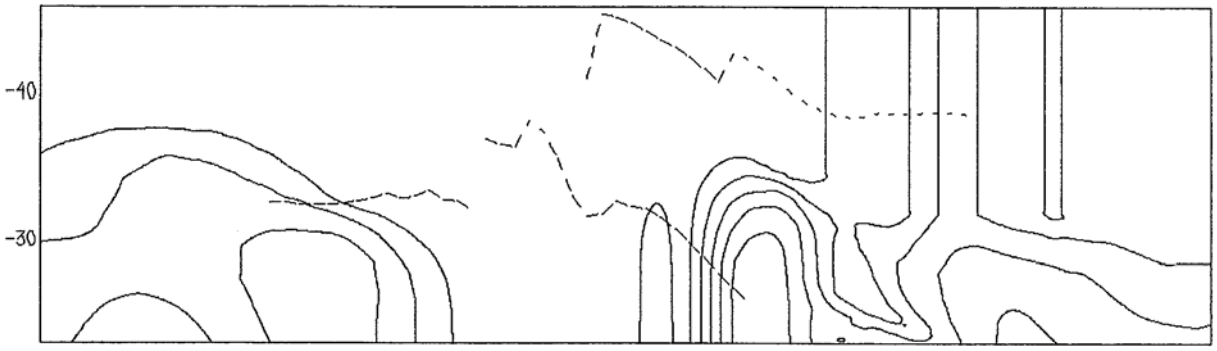

Figure 1(b) Shows contours of relative humidity with temperature as the vertical coordinate. Also shows correlation surface ridges from fig 1(c)

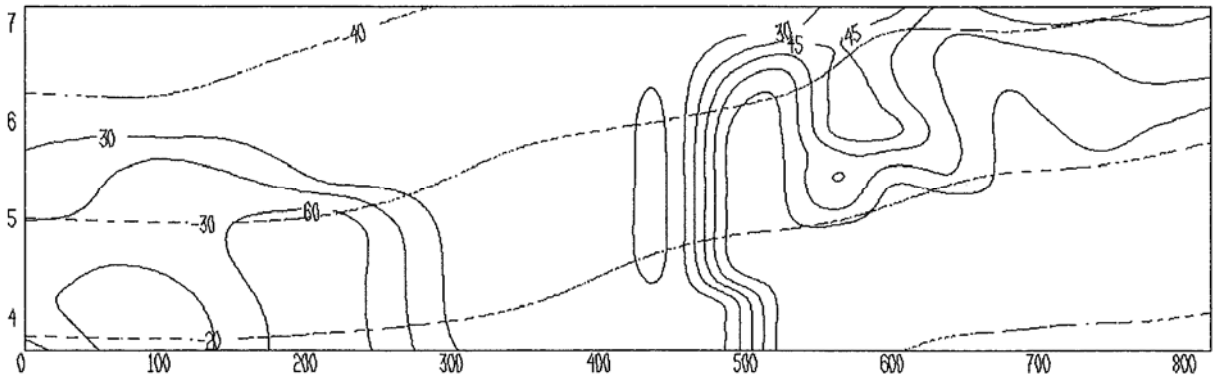

Figure 1(a) Shows contours of relative humidity (continuous) and temperature (dashed) with height as the vertical coordinate for IOP8RUN3

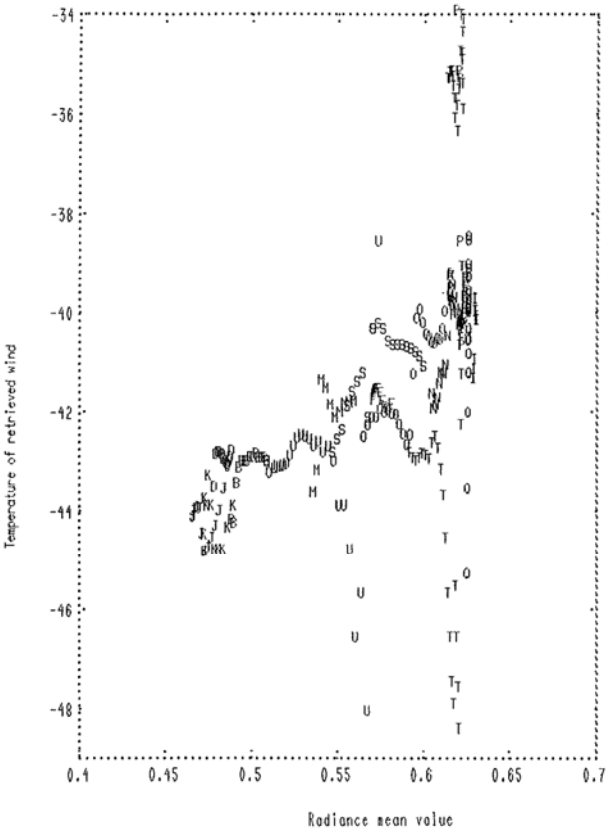

Figure 2(a). Plot of temperature of retrieved wind against radiance without data selection

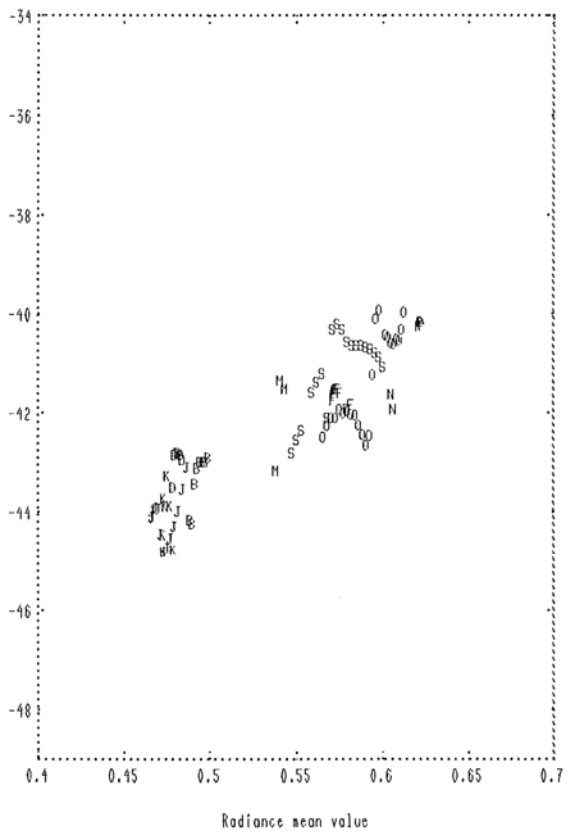

Figure 2(b). As figure 2(a) but data selected as described in text

References

Eigenwillig, N and Fischer, H. (1982) Determination of midtropospheric wind vectors by tracking pure water vapour structures in METEOSAT water vapour image sequences. *Bull. Amer. Met. Soc.* **63** 44-58

ESOC (1989) Annexe to the METEOSAT-4 calibration report *OD/MEP/MET(July 1989), Available from Meteosat Exploitation Project, ESOC*

Laurent, H. (1991) Wind extraction from METEOSAT water vapour channel image data. *Jour Appl Met,* **32** pp 1124 - 1133

Lunnon, R.W., Lowe, D.A. Barnes, J.A. and Dharssi.I. (1992) Study of cirrus cloud winds: analysis of ICE data. *Proceedings of 9th METEOSAT Scientific Users' Meeting, Locarno, September 1992, published by EUMETSAT*

Szantai, A. (1991) Wind extraction and validation from the water vapour channel of METEOSAT during the Internatinal Cirrus Experiment. *Proceedings of a workshop on wind extraction from operational meeorological satellite data (published by EUMETSAT)* 63-70

Thorpe, A.J. and Clough, S.A. (1991) Meososcale dynamics of cold fronts: structures described by dropsoundings in FRONTS87. *Quart Journ Roy Met Soc* **117** 903-942